Structural Characterization of the UV-Induced Fragmentation Products in an Ion Trap by Infrared Multiple Photon Dissociation Spectroscopy

ARTICLE *in* JOURNAL OF PHYSICAL CHEMISTRY LETTERS · DECEMBER 2013

Impact Factor: 7.46 · DOI: 10.1021/jz402348n

5 AUTHORS, INCLUDING:

Scuderi Debora
Université Paris-Sud 11
72 PUBLICATIONS **1,015** CITATIONS
SEE PROFILE

Valeria Lepère
Université Paris-Sud 11
19 PUBLICATIONS **203** CITATIONS
SEE PROFILE

Giovanni Piani
32 PUBLICATIONS **256** CITATIONS
SEE PROFILE

Anne Zehnacker
French National Centre for Scientific Research
92 PUBLICATIONS **1,645** CITATIONS
SEE PROFILE

THE JOURNAL OF PHYSICAL CHEMISTRY Letters

Letter

pubs.acs.org/JPCL

Structural Characterization of the UV-Induced Fragmentation Products in an Ion Trap by Infrared Multiple Photon Dissociation Spectroscopy

Debora Scuderi,*[,†] Valeria Lepere,[‡] Giovanni Piani,[‡] Aude Bouchet,[‡] and Anne Zehnacker-Rentien*[,‡]

[†]Laboratoire de Chimie Physique and [‡]Institut des Sciences Moléculaires d'Orsay, Université Paris-Sud, CNRS, F-91405 Orsay, France

Supporting Information

ABSTRACT: Protonated cinchona alkaloids and their dimers undergo photochemical reaction in the gas phase, leading to UV-specific photofragments, not observed by collision-induced dissociation. Simultaneous coupling of UV and IR lasers with a Paul ion trap has been achieved for obtaining the vibrational spectrum of the fragments arising from the photodissociation. The structure of the photoproduced radical has been fully characterized by comparing the experimental spectrum to that simulated by DFT calculations.

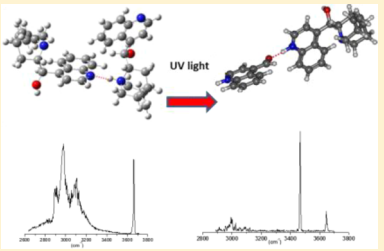

SECTION: Spectroscopy, Photochemistry, and Excited States

Mass spectrometry coupled with UV-induced photofragmentation (UVPD) of biomolecules has recently attracted much attention in the field of structural characterization of gas-phase peptide cations, metallocenes, glycolipids, or other biologically relevant ionic systems.[1−8] Besides the interest of such studies in the context of the photostability of the elementary blocks of life, UVPD offers promising possibilities in the field of top-down protein characterization because it leads to specific fragments that are not observed by collision-induced dissociation (CID).[9] The specific UV-induced fragmentation channels are also used as an elegant tool for recording the electronic spectrum (action spectrum) of protonated amino acids or peptides in cold ion traps.[10,11]

Cinchona alkaloids are well-suited for studies combining mass spectrometry and UVPD as they possess a chromophore in the near-UV, the quinoline, and a complex side chain, the alkaloid bicycle. Moreover, the structure of neutral and protonated cinchona alkaloids is well-known in solution as well as in the gas phase.[12−16] The most simple cinchona alkaloid, cinchonidine (Cd), is shown in Scheme 1. The protonated molecule CdH^+ as well as the protonated dimer $(Cd)_2H^+$, isolated in an ion trap, have been spectroscopically characterized by infrared multiple photon dissociation (IRMPD).[17] The monomer is protonated on the alkaloid ring nitrogen N_1 and retains the conformation of the neutral molecule. It shows an open-type structure with little interaction between the alkaloid and the aromatic frame. The two similar low-energy conformers that have been evidenced experimentally only differ by the presence, or not, of a $NH^+\cdots O$ interaction (Figure 1a and b, respectively). The most stable structure of the dimer, shown in Figure 1c, involves a very strong hydrogen bond between the protonated monomer and the aromatic nitrogen N_{arom} of the neutral moiety.[17] A less stable form is held by two hydrogen bonds of lesser strength (Figure 1d). The $(Cd)_2H^+$ dimer has been shown to undergo UV-induced fragmentation, leading to specific photofragments.[18]

UVPD of $(Cd)_2H^+$ (m/z 589) shows two dissociation paths. The first one, common to CID, is the loss of neutral Cd (m 294) and protonated CdH^+ (m/z 295) monomers. In addition, there is a new fragmentation channel, unique to UVPD, which consists of the loss of the neutral alkaloid radical $Nu^\bullet$ (m 136), with concomitant detection of a radical cation (m/z 453). The postulated mechanism, schematically described in Scheme 2, is supposed to involve fast excited-state proton transfer (ESPT) within the dimer. The migration of the proton from N_1 to N_{arom} is accompanied by the cleavage of the C_8-C_9 bond and loss of the alkaloid radical.[18] It is to be noted at this stage that the UVPD process at play in the dimer strongly differs from that of the monomer. Indeed, UVPD of CdH^+ results in the loss of the protonated alkaloid (m/z 137) or the alkaloid cation (m/z

Scheme 1. (−)−Cinchonidine (Cd) (1S,3R,4S,8S,9R)

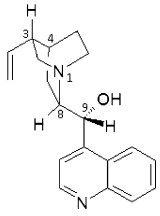

Received: October 31, 2013
Accepted: December 4, 2013
Published: December 4, 2013

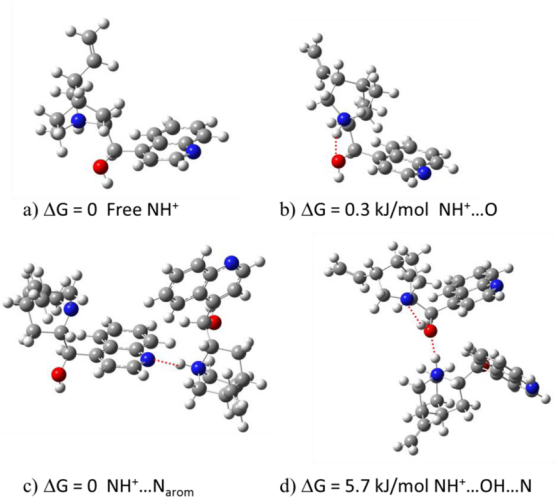

Figure 1. Most stable calculated structures of CdH^+ with no $NH^+\cdots O$ intramolecular hydrogen bond (a) or with an $NH^+\cdots O$ intramolecular hydrogen bond (b). Most stable calculated structures of $(Cd)_2H^+$ (c,d). ΔG is the calculated free energy relative to the most stable protonated monomer or dimer, respectively. All of these structures have been calculated at the B3-LYP/6-311+G** level.[17]

Scheme 2. Proposed Schematic Mechanism for the UVPD Reaction in $(Cd)_2H^+$

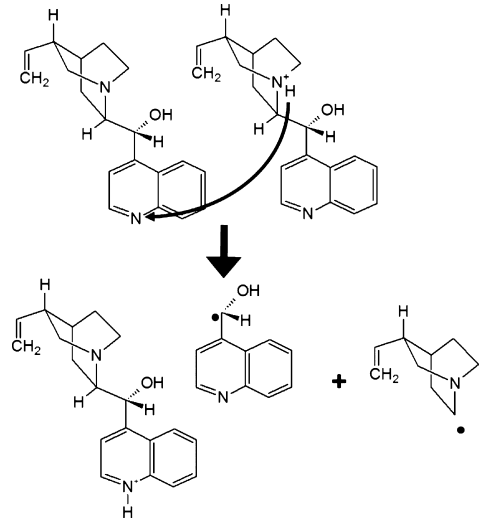

136).[19] The loss of m/z 136 is supposed to happen through conical intersection between the optically excited state and a $\pi-\sigma^*$ state localized on the N_1H^+ bond, leading to H loss and concomitant C_8-C_9 cleavage.[19] The $\pi-\sigma^*$ state is similar to that responsible for H atom loss in heteroatom-substituted aromatic molecules like phenol.[20,21] It also plays a role in the UVPD of protonated amino acids where it explains the loss of a H atom accompanied by a $C_\alpha-C_\beta$ cleavage.[1,22]

To confirm the mechanism postulated for UVPD of the dimer, the structure of the UV photofragment must be determined, which is the subject of this Letter. To this aim, we can resort first to MS^3 experiments, which have been used already for determining the structure of radicals produced by CID of peptides.[23] However, CID is usually described within the frame of statistical reactions by means of the RRKM model.[24] As a result, the fragments obtained by CID of a noncovalent dimer arise from the dissociation of the weakest bond, the intermolecular one, and usually correspond to the monomers. CID of the m/z 453 photofragment leads to the observation of the m/z 295 CdH^+ fragment (Figure 2). The

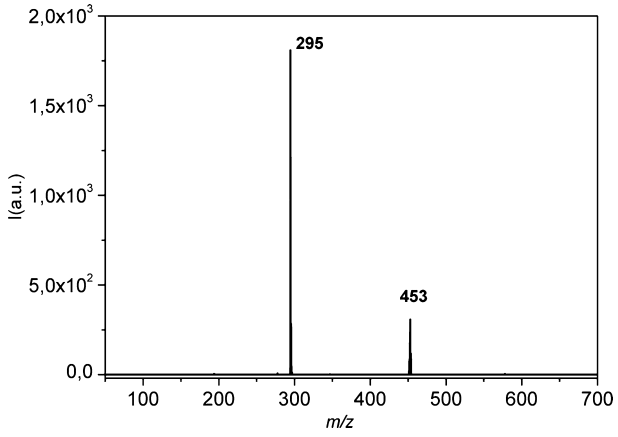

Figure 2. CID-MS^2 mass spectra of the m/z 453 radical cation arising from the photodissociation of $(Cd)_2H^+$, recorded with a radio frequency amplitude of 0.25.

only structural information gained from this experiment is that the charge in the radical cation product is borne by a CdH^+ subunit and not by the remaining $(Cd-Nu^\bullet)$ hydroxyalkyl radical moiety. Vibrational spectroscopy as obtained by IRMPD provides an elegant alternative for structural characterization. It has been widely used for determining the structure of gas-phase ions or ionic complexes.[25] In the field of chemical reactivity, it has been applied for defining the nature of reaction products[26] or the structure of ion radicals.[27] It has also allowed structural characterization of the fragments arising from CID or electron capture dissociation (ECD) of peptides in MS^3 experiments.[28−31] However, no IRMPD spectroscopy of photoproducts has been reported so far because of the technical difficulties of such experiments, requiring a MS^3 scheme coupled with a UV and a powerful IR laser.

We describe here the first IRMPD characterization of the product of a UVPD reaction in the gas phase, using a Paul ion trap coupled to a UV laser and either a free electron laser (FEL) or an OPO as the IR source. The experiments rest on a modified MS^3 scheme in a Paul ion trap.[32] The parent protonated cinchonidine dimer, $(Cd)_2H^+$ (m/z 589), has been isolated and fragmented by irradiation at 266 nm. The resulting ionic photofragment (m/z 453) has been isolated in a second step; its vibrational spectrum has been recorded by IRMPD spectroscopy.

The most striking result is the strong difference between the photofragment spectrum and that of the parent, emphasized in Figure 3 for the near-IR region. The parent spectrum shows an intense and narrow band at 3669 cm^{-1}, assigned to the indiscernible free ν(OH) stretches of the two Cd subunits. The broader absorption bands observed in the ν(NH) stretch region have been interpreted in terms of the coexistence of two main isomers of the dimer, shown in Figure 1c and d.[17] In both dimers, the proton is borne by the alkaloid nitrogen N_1 of one of the molecules. The most stable dimer (Figure 1c) involves a very strong hydrogen bond between N_1H^+ of the protonated monomer and the aromatic nitrogen N_{arom} of the neutral moiety, the strongly interacting $\nu(N_1H)$ stretch being responsible for the broad absorption below 2900 cm^{-1}. A less stable form (Figure 1d) is stabilized by two hydrogen bonds of

dx.doi.org/10.1021/jz402348n | J. Phys. Chem. Lett. 2014, 5, 56−61

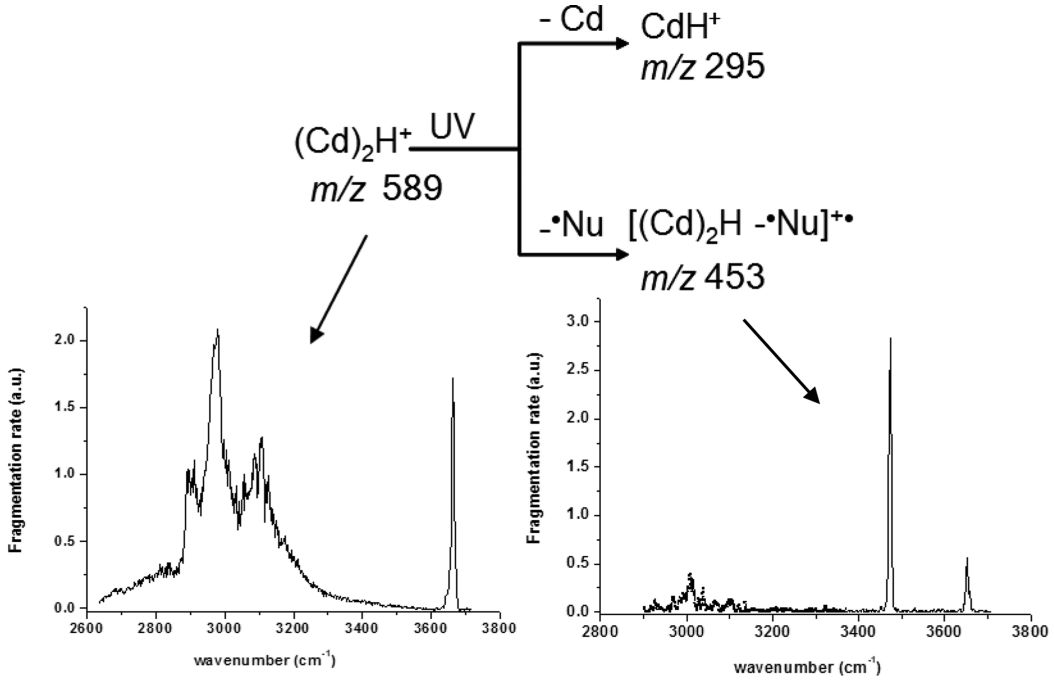

Figure 3. IRMPD spectra of the $(Cd)_2H^+$ parent (m/z 589, left) and of the photofragment (m/z 453, right), in the near-IR region.

lesser strength, namely, a hydrogen bond from the N_1H^+ of the protonated moiety to the OH of the neutral one, which in turn acts as a donor in an intramolecular OH···N interaction. This structure accounts for the bound ν(OH) and ν(NH) stretches observed at 3107 and 2978 cm^{-1}, respectively.[17] In contrast, the spectrum of the m/z 453 fragment shows two distinct peaks, a free ν(OH) stretch at 3646 cm^{-1} and an intense narrow band located at 3467 cm^{-1} (Figure 3). The former is characteristic of a free ν(OH) stretch, either that of CdH^+,[17] or that of a hydroxyalkyl radical.[33] The latter, which is the most intense band of the spectrum, is out of the expected range for the $\nu(N_1H)$ stretch localized on the protonated alkaloid; a free $\nu(N_1H)$ stretch would be expected to appear near 3300 cm^{-1}.[17] Furthermore, the broad band due to the bound $\nu(N_1H)$ stretch observed for $(Cd)_2H^+$ in the 3000 cm^{-1} region has disappeared in the photofragment. This indicates that the protonation site of the photofragment is not the alkaloid nitrogen N_1. This observation, together with the narrow bandwidth of the 3467 cm^{-1} band, suggests assigning the 3467 cm^{-1} band to the $\nu(N_{arom}H)$ stretch of a radical cation complex protonated on the quinoline nitrogen. Indeed, there is similarity between the photofragment spectrum in the fingerprint region (Figure 4), with a very strong band at around 1580 cm^{-1}, and that reported for protonated quinoline.[34]

A definitive assignment can be proposed on the basis of DFT calculations at the b97D/TZVPP level of theory using the Turbomole 6.3 package.[35−37] Conformational searching and geometry optimization of the radical fragment formed by proton transfer followed by C_8−C_9 dissociation of the dimer has led to four main classes of products. The first family in which the proton is not located on Cd can be discarded a priori because it does not agree with the CID results shown in Figure 2 (loss of m/z 295). The second class where the proton is located on the alkaloid nitrogen N_1 can be discarded as well because the simulated spectrum does not agree with the experimental one, as shown in the Supporting Information. We are thus left with two radical fragments, namely R_I and R_{II},

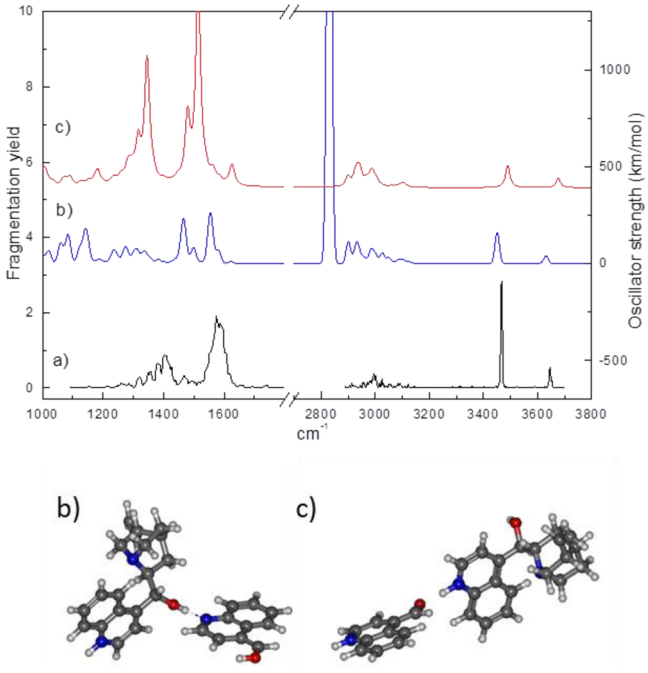

Figure 4. (Top) Comparison between the experimental (a) and simulated (b,c) vibrational spectra. (Bottom) Calculated structures of the photofragments (m/z 453) R_I (b) and R_{II} (c) arising from the UVPD of $(Cd)_2H^+$.

shown in Figure 4b and c, respectively, together with their simulated IR spectra. Both of them show protonation on the Cd quinoline ring N_{arom} and are thus compatible with the CID results. Both simulated spectra, obtained by convoluting the harmonic frequencies scaled by 0.98 with a 10 cm^{-1} width Gaussian band shape, show nice agreement with the experiment in the 3 μm region. Indeed, the strongest bands observed in the 3 μm region can be readily assigned to the radical free ν(OH) stretch calculated at 3631 and 3675 cm^{-1} (scaled value) for R_I

dx.doi.org/10.1021/jz402348n | J. Phys. Chem. Lett. 2014, 5, 56−61

and R_{II} and to the free aromatic ν(NH) stretch calculated at 3451 and 3490 cm^{-1} for R_I and R_{II}, respectively. Both structures involve a strong O···H···N_{arom} hydrogen bonding interaction but differ in their nature. R_I shows a OH···N_{arom} hydrogen bond involving the OH of the CdH^+ and the N_{arom} of the quinoline radical, the OH of the hydroxyalkyl part remaining free. Its binding energy including zero-point energy corrections amounts to 48 kJ/mol. The OH···N_{arom} hydrogen bond length amounts to 1.55 Å, and the bound ν(OH) stretch is calculated at 2839 cm^{-1}. In contrast, the O···H···N_{arom} hydrogen bond in R_{II} involves the OH group of the hydroxyalkyl radical, that of CdH^+ being free. The proton has migrated from the hydroxyalkyl radical to N_{arom}, and the bound ν(NH) stretch is calculated at 2309 cm^{-1}. In addition to the fact that strongly bound ν(OH) or ν(NH) stretches are usually difficult to evidence because of their inherent breadth,[38,39] these values are out of the range of both the OPO and FEL used here, and the spectrum could not be recorded in this range.

The fingerprint region of R_I and R_{II} shows satisfactory agreement with the calculations. The most intense peak observed in the experimental spectrum at around 1580 cm^{-1} can be assigned to the modes calculated at 1552/1558 cm^{-1} in R_I, which correspond to coupled β($N_{arom}H^+$) and β(CH) bending motions or to those at 1479/1513/1517 cm^{-1} in R_{II}, which are due to coupled β($N_{arom}H^+$) or β(NH···O) and β(CH) bends. The other prominent band at 1410 cm^{-1} can correspond to the intense bonded β(OH) coupled with β(CH) bends calculated at 1499/1469/1461 cm^{-1} in R_I. It can also correspond to intense transitions involving complex β(OH), β(NH), and β(CH) bending motions calculated at 1341/1344/1350/1366 cm^{-1} in R_{II}. Although both simulated spectra are compatible with the experiment, the match is better for R_{II}. Moreover, R_{II} is more stable than R_I by 90 kJ/mol. The observed radical fragment has been therefore tentatively assigned to R_{II}.

These spectroscopic results confirm the assignment of the photofragment to a radical cation protonated on the aromatic nitrogen of the CdH^+ moiety and allow proposing a UVPD mechanism. One has to take into account that the dimer can be excited on either its neutral or protonated moiety. Excitation of the neutral part results in the increase of the basicity of its N_{arom}, which undergoes proton transfer from the protonated moiety. Indeed, the most basic site of Cd in the electronic ground state is the alkaloid N_1 with an associated pK_A higher than that of the aromatic nitrogen N_{arom} (9.7 versus 5.7), but it is the opposite in the S_1 state where the pK_A of N_{arom} increases to 11−12. The proton-transferred dimer either dissociates by internal conversion (IC) or undergoes back proton transfer followed by dissociation. In both cases, CdH^+ (m/z 295) is produced. In contrast, excitation of the protonated part results in H atom loss from N_1H^+, as observed in the CdH^+ monomer. In the most stable structure of $(Cd)_2H^+$ shown in Figure 1, N_1H^+ is involved in a strong N_1H^+···N_{arom} hydrogen bond, and the H atom loss is accompanied by an electron transfer. The resulting process consists of a proton transfer from N_1H^+ of the protonated moiety to N_{arom} of the neutral one, with concomitant C_8−C_9 cleavage. It should be noted that the optically excited $(Cd)_2H^+$ is prepared in a geometry that facilitates proton transfer as the proton has only to move a small distance from N_1 to N_{arom}.

In conclusion, we report here a new spectroscopic tool for probing the nature of the products of photofragmentation of ions. The experiments described in this Letter open the way to the study of numerous aspects of the photochemistry of cinchona alkaloids, in particular, the effects of stereochemistry and chirality, which are in progress.[17,18,40] Moreover, UV-specific and sometimes isomer-selective photofragments have also been observed in the case of protonated polypeptides. The same kind of studies can therefore be applied to this class of molecules to provide very useful structural and excited-state dynamics information.

EXPERIMENTAL METHODS

The experiments rest on a modified MS^3 scheme in a Paul ion trap (Bruker, Esquire 3000+),[32] equipped with a CaF_2 entrance window. Ions were generated by an electrospray source. The ESI conditions were as follows: flow rate of 150 μL/h, drying gas flow of 5 L/mn, nebulizer pressure of 3.5 bar, capillary voltage of −4500 V, and drying gas temperature of 200 °C. The photodissociation was induced by the fourth harmonic of a 10 Hz Nd:YAG laser (Minilite Continuum, 500 μJ/pulse) slightly focused by a 1000 mm focal length lens to the center of the trap. The IRMPD spectra of the photofragments were recorded using the CLIO (Centre Laser Infrarouge d'Orsay) IR FEL, focused at the center of the trap by a ZnSe 400 mm focal length lens, or a tabletop IR optical parametric oscillator/amplifier (OPO/OPA) (LaserVision), focused by a 250 mm focal length CaF_2 lens, to cover the 1100−1800 or 2750−3750 cm^{-1} spectral range, respectively.

Infrared spectra have been obtained by monitoring the abundance of the parent (m/z 453) and that of the fragment ion (CdH^+ m/z 295). The fragmentation yield used for plotting the IRMPD spectrum is defined as $Q = -\ln(P/(F+P))$ as a function of the IR wavenumber, where P and F stand for the parent and the fragment, respectively. The MS^3 sequence has been obtained as follows: the parent protonated cinchonidine dimer, $(Cd)_2H^+$ (m/z 589), has been mass selected in a 5 Da window and fragmented by irradiation at 266 nm for 1 s. The resulting ionic photofragment (m/z 453) has been isolated in a second step; its vibrational spectrum has been recorded by IRMPD with 1 s of irradiation time by monitoring the CdH^+ (m/z 295) loss channel.

ASSOCIATED CONTENT

Supporting Information

Comparison between the experimental and simulated vibrational spectra and calculated structures of the photofragments arising from the UVPD of $(Cd)_2H^+$. This material is available free of charge via the Internet at http://pubs.acs.org.

AUTHOR INFORMATION

Corresponding Authors

*E-mail: debora.scuderi@u-psud.fr. Fax: +33169156188. Tel: +33169157574 (D.S.).

*E-mail: anne.zehnacker-rentien@u-psud.fr. Fax: +33169156777. Tel: +33169153933 (A.Z.-R.).

Notes

The authors declare no competing financial interest.

ACKNOWLEDGMENTS

The mass spectrometry platform SMAS of the Laboratoire de Chimie Physique (University Paris-Sud) is gratefully acknowledged. We thank Dr. J. M. Ortega and the CLIO team for technical assistance. We acknowledge Y. Peperstraete, V. Steinmetz, C. Le Bris, Ch. Lefumeux, and Dr. B. Lucas for

their assistance in the experimental work. We acknowledge the use of the computing facility cluster GMPCS of the LUMAT federation (FR LUMAT 2764).

REFERENCES

(1) Lucas, B.; Barat, M.; Fayeton, J. A.; Perot, M.; Jouvet, C.; Gregoire, G.; Nielsen, S. B. Mechanisms of Photoinduced C-Alpha-C-Beta Bond Breakage in Protonated Aromatic Amino Acids. *J. Chem. Phys.* **2008**, *128*, 164302.
(2) Joly, L.; Antoine, R.; Broyer, M.; Dugourd, P.; Lemoine, J. Specific UV Photodissociation of Tyrosyl-Containing Peptides in Multistage Mass Spectrometry. *J. Mass Spectrom.* **2007**, *42*, 818−824.
(3) Reilly, J. P. Ultraviolet Photofragmentation of Biomolecular Ions. *Mass Spectrom. Rev.* **2009**, *28*, 425−447.
(4) O'Brien, J. P.; Brodbelt, J. S. Structural Characterization of Gangliosides and Glycolipids via Ultraviolet Photodissociation Mass Spectrometry. *Anal. Chem.* **2013**, *85*, 10399−10407.
(5) Lin, C. Y.; Dunbar, R. C. Time-Resolved Photodissociation of Gas-Phase Nickelocene Cation — Determination of Bond Strength and Radiative Relaxation Rate. *J. Phys. Chem.* **1995**, *99*, 1754−1759.
(6) Kirk, B. B.; Trevitt, A. J.; Blanksby, S. J.; Tao, Y.; Moore, B. N.; Julian, R. R. Ultraviolet Action Spectroscopy of Iodine Labeled Peptides and Proteins in the Gas Phase. *J. Phys. Chem. A* **2013**, *117*, 1228−1232.
(7) Guan, Z. Q.; Kelleher, N. L.; Oconnor, P. B.; Aaserud, D. J.; Little, D. P.; McLafferty, F. W. 193 Nm Photodissociation of Larger Multiply-Charged Biomolecules. *Int. J. Mass Spectrom. Ion Processes* **1996**, *157*, 357−364.
(8) Moon, J. H.; Shin, Y. S.; Cha, H. J.; Kim, M. S. Photo Dissociation at 193 nm of Some Singly Protonated Peptides and Proteins with m/z 2000−9000 Using a Tandem Time-of-Flight Mass Spectrometer Equipped with a Second Source for Delayed Extraction/Post-Acceleration of Product Ions. *Rapid Commun. Mass Spectrom.* **2007**, *21*, 359−368.
(9) Shaw, J. B.; Li, W.; Holden, D. D.; Zhang, Y.; Griep-Raming, J.; Fellers, R. T.; Early, B. P.; Thomas, P. M.; Kelleher, N. L.; Brodbelt, J. S. Complete Protein Characterization Using Top-Down Mass Spectrometry and Ultraviolet Photodissociation. *J. Am. Chem. Soc.* **2013**, *135*, 12646−12651.
(10) Stearns, J. A.; Guidi, M.; Boyarkin, O. V.; Rizzo, T. R. Conformation-Specific Infrared and Ultraviolet Spectroscopy of Tyrosine-Based Protonated Dipeptides. *J. Chem. Phys.* **2007**, *127*, 154322.
(11) Redwine, J. G.; Davis, Z. A.; Burke, N. L.; Oglesbee, R. A.; McLuckey, S. A.; Zwier, T. S. A Novel Ion Trap Based Tandem Mass Spectrometer for the Spectroscopic Study of Cold Gas Phase Polyatomic Ions. *Int. J. Mass Spectrom.* **2013**, *348*, 9−14.
(12) Burgi, T.; Baiker, A. Conformational Behavior of Cinchonidine in Different Solvents: A Combined NMR and Ab Initio Investigation. *J. Am. Chem. Soc.* **1998**, *120*, 12920−12926.
(13) Sen, A.; Bouchet, A.; Lepere, V.; Le Barbu-Debus, K.; Scuderi, D.; Piuzzi, F.; Zehnacker-Rentien, A. Conformational Analysis of Quinine and Its Pseudo Enantiomer Quinidine: A Combined Jet-Cooled Spectroscopy and Vibrational Circular Dichroism Study. *J. Phys. Chem. A* **2012**, *116*, 8334−8344.
(14) Olsen, R. A.; Borchardt, D.; Mink, L.; Agarwal, A.; Mueller, L. J.; Zaera, F. Effect of Protonation on the Conformation of Cinchonidine. *J. Am. Chem. Soc.* **2006**, *128*, 15594−15595.
(15) Lai, J. F.; Ma, Z.; Mink, L.; Mueller, L. J.; Zaera, F. Influence of Peripheral Groups on the Physical and Chemical Behavior of Cinchona Alkaloids. *J. Phys. Chem. B* **2009**, *113*, 11696−11701.
(16) Bürgi, T.; Vargas, A.; Baiker, A. VCD Spectroscopy of Chiral Cinchona Modifiers Used in Heterogeneous Enantioselective Hydrogenation: Conformation and Binding of Non-Chiral Acids. *J. Chem. Soc., Perkin Trans. 2* **2002**, 1596−1601.
(17) Scuderi, D.; Le Barbu-Debus, K.; Zehnacker, A. The Role of Weak Hydrogen Bonds in Chiral Recognition. *Phys. Chem. Chem. Phys.* **2011**, *13*, 17916−17929.
(18) Scuderi, D.; Maitre, P.; Rondino, F.; Le Barbu-Debus, K.; Lepere, V.; Zehnacker-Rentien, A. Chiral Recognition in Cinchona Alkaloid Protonated Dimers: Mass Spectrometry and UV Photodissociation Studies. *J. Phys. Chem. A* **2010**, *114*, 3306−3312.
(19) Kumir, S.; Lucas, B.; Scuderi, D.; Lepere, V.; Le Barbu-Debus, K.; Zehnacker, A. To Be Published.
(20) Sobolewski, A. L.; Domcke, W.; Dedonder-Lardeux, C.; Jouvet, C. Excited-State Hydrogen Detachment and Hydrogen Transfer Driven by Repulsive $^1\pi-\Sigma^*$ States: A New Paradigm for Nonradiative Decay in Aromatic Biomolecules. *Phys. Chem. Chem. Phys.* **2002**, *4*, 1093−1100.
(21) Roberts, G. M.; Williams, C. A.; Yu, H.; Chatterley, A. S.; Young, J. D.; Ullrich, S.; Stavros, V. G. Probing Ultrafast Dynamics in Photoexcited Pyrrole: Timescales for $^1\pi-\Sigma^*$ Mediated H-Atom Elimination. *Faraday Discuss.* **2013**, *163*, 95−116.
(22) Perot, M.; Lucas, B.; Barat, M.; Fayeton, J. A.; Jouvet, C. Mechanisms of UV Photodissociation of Small Protonated Peptides. *J. Phys. Chem. A* **2010**, *114*, 3147−3156.
(23) Bernier, M. C.; Paizs, B.; Wysocki, V. H. Influence of a Gamma Amino Acid on the Structures and Reactivity of Peptide a_3 Ions. *Int. J. Mass Spectrom.* **2012**, *316*, 259−267.
(24) Forst, W. *Theory of Unimolecular Reactions*; Academic Press: New York, 1973.
(25) Polfer, N. C. Infrared Multiple Photon Dissociation Spectroscopy of Trapped Ions. *Chem. Soc. Rev.* **2011**, *40*, 2211−2221.
(26) Lanucara, F.; Chiavarino, B.; Crestoni, M. E.; Scuderi, D.; Sinha, R. K.; Maitre, P.; Fornarini, S. S-Nitrosation of Cysteine as Evidenced by IRMPD Spectroscopy. *Int. J. Mass Spectrom.* **2012**, *330*, 160−167.
(27) Osburn, S.; Steill, J. D.; Oomens, J.; O'Hair, R. A. J.; van Stipdonk, M.; Ryzhov, V. Structure and Reactivity of the Cysteine Methyl Ester Radical Cation. *Chem.—Eur. J.* **2011**, *17*, 873−879.
(28) Oomens, J.; Steill, J. D. The Structure of Deprotonated Tri-Alanine and Its a_3^- Fragment Anion by IR Spectroscopy. *J. Am. Soc. Mass Spectrom.* **2010**, *21*, 698−706.
(29) Frison, G.; van der Rest, G.; Turecek, F.; Besson, T.; Lemaire, J.; Maitre, P.; Chamot-Rooke, J. Structure of Electron-Capture Dissociation Fragments from Charge-Tagged Peptides Probed by Tunable Infrared Multiple Photon Dissociation. *J. Am. Chem. Soc.* **2008**, *130*, 14916−+.
(30) Durand, S.; Rossa, M.; Hernandez, O.; Paizs, B.; Maitre, P. Ir Spectroscopy of b_4 Fragment Ions of Protonated Pentapeptides in the X−H (X = C, N, O) Region. *J. Phys. Chem. A* **2013**, *117*, 2508−2516.
(31) Wassermann, T. N.; Boyarkin, O. V.; Paizs, B.; Rizzo, T. R. Conformation-Specific Spectroscopy of Peptide Fragment Ions in a Low-Temperature Ion Trap. *J. Am. Soc. Mass Spectrom.* **2012**, *23*, 1029−1045.
(32) Mac Aleese, L.; Simon, A.; McMahon, T. B.; Ortega, J.-M.; Scuderi, D.; Lemaire, J.; Maître, P. Mid-IR Spectroscopy of Protonated Leucine Methyl Ester Performed with an FTICR or a Paul Type Ion-Trap. *Int. J. Mass Spectrom.* **2006**, *249−250*, 14−20.
(33) Feng, L.; Wei, J.; Reisler, H. Rotationally Resolved Infrared Spectroscopy of the Hydroxymethyl Radical (CH_2OH). *J. Phys. Chem. A* **2004**, *108*, 7903−7908.
(34) Galue, H. A.; Pirali, O.; Oomens, J. Gas-Phase Infrared Spectra of Cationized Nitrogen-Substituted Polycyclic Aromatic Hydrocarbons. *Astron. Astrophys.* **2010**, 517.
(35) Ahlrichs, R.; Bar, M.; Haser, M.; Horn, H.; Kolmel, C. Electronic-Structure Calculations on Workstation Computers — The Program System Turbomole. *Chem. Phys. Lett.* **1989**, *162*, 165−169.
(36) Antony, J.; Grimme, S. Density Functional Theory Including Dispersion Corrections for Intermolecular Interactions in a Large Benchmark Set of Biologically Relevant Molecules. *Phys. Chem. Chem. Phys.* **2006**, *8*, 5287−5293.
(37) Schafer, A.; Huber, C.; Ahlrichs, R. Fully Optimized Contracted Gaussian-Basis Sets of Triple Zeta Valence Quality for Atoms Li to Kr. *J. Chem. Phys.* **1994**, *100*, 5829−5835.
(38) Bakker, J. M.; Sinha, R. K.; Besson, T.; Brugnara, M.; Tosi, P.; Salpin, J. Y.; Maitre, P. Tautomerism of Uracil Probed via Infrared

Spectroscopy of Singly Hydrated Protonated Uracil. *J. Phys. Chem. A* **2008**, *112*, 12393−12400.
(39) Seurre, N.; Le Barbu-Debus, K.; Lahmani, F.; Zehnacker-Rentien, A.; Sepiol, J. Electronic and Vibrational Spectroscopy of Jet-Cooled *m*-Cyanophenol and Its Dimer: Laser-Induced Fluorescence and Fluorescence-Dip IR Spectra in the S_0 and S_1 States. *Chem. Phys.* **2003**, *295*, 21−33.
(40) Zehnacker, A.; Suhm, M. A. Chirality Recognition between Neutral Molecules in the Gas Phase. *Angew. Chem., Int. Ed.* **2008**, *47*, 6970−6992.

dx.doi.org/10.1021/jz402348n | *J. Phys. Chem. Lett.* 2014, 5, 56−61